

An epidemiological compartmental model with automated parameter estimation and forecasting of the spread of COVID-19 with analysis of data from Germany and Brazil

Adriano A. Batista^{1*} and Severino Horácio da Silva^{2†}

¹ *Departamento de Física, Universidade Federal de*

Campina Grande, 58051-900 Campina Grande PB, Brazil.

² *Departamento de Matemática, Universidade Federal de Campina Grande,*

58051-900 Campina Grande PB, Brazil.

(Dated: August 2, 2021)

In this work, we adapt the epidemiological SIR model to study the evolution of the dissemination of COVID-19 in Germany and Brazil (nationally, in the State of Paraíba, and in the City of Campina Grande). We prove the well posedness and the continuous dependence of the model dynamics on its parameters. We also propose a simple probabilistic method for the evolution of the active cases that is instrumental for the automatic estimation of parameters of the epidemiological model. We obtained statistical estimates of the active cases based the probabilistic method and on the confirmed cases data. From this estimated time series we obtained a time-dependent contagion rate, which reflects a lower or higher adherence to social distancing by the involved populations. By also analysing the data on daily deaths, we obtained the daily lethality and recovery rates. We then integrate the equations of motion of the model using these time-dependent parameters. We validate our epidemiological model by fitting the official data of confirmed, recovered, death, and active cases due to the pandemic with the theoretical predictions. We obtained very good fits of the data with this method. The automated procedure developed here could be used for basically any population with a minimum of extra work. Finally, we also propose and validate a forecasting method based on Markov chains for the evolution of the epidemiological data for up to two weeks.

* adriano@df.ufcg.edu.br

† horacio@mat.ufcg.edu.br

I. INTRODUCTION

The COVID-19 pandemic already has reached practically the whole planet. According to the World Health Organization (WHO, Situation Report-41 [1]), although around 80% of the infected people present mild symptoms (equivalent to the common flu), older people and those with a history of other diseases like diabetes, cardiovascular, and chronic respiratory syndrome can develop serious problems after being infected by the SARS-CoV-2 virus. It was first identified in December 2019 in the City of Wuhan, Province of Hubei, China. From there it spread across Asia, Europe, and the other continents [2]. On March 11th, the WHO declared it to be a pandemic [3].

In this work, we investigate the spread of the pandemic in 4 different scenarios: Germany, Brazil, the Brazilian State of Paraíba, and the City of Campina Grande. We use the data from Germany mostly as a benchmark test for our model, since very likely their COVID-19 data is one of the most accurate in the world, which is due to the widespread testing of its population. Furthermore, the social distancing, isolation, and use of personal protection equipment (PPE) there has been far more efficient than the measures taken in Brazil in containing the spread of COVID-19 infections.

The first confirmed case in Brazil occurred in February 25th of 2020, when a 61-year-old man who had returned from Italy tested positive and the first death due to the pandemic occurred on March 12. It is very unlikely all cases of COVID-19 contaminations evolved from this patient. As reported in other countries, there were multiple imported infections, which usually drive the contagion rate to very high values in the initial stages of the epidemic. In Brazil and in the majority of countries around the world social distancing policies have been adopted in order to decrease the rate of contagion and thus allow that health systems do not collapse and have conditions to treat the gravest cases of the disease.

In the State of Paraíba, according to the Paraíba Department of Health, the first confirmed case of COVID-19 was registered on March 18th of 2020. It was a man who lived in the City of João Pessoa that had returned from a trip to Europe on February 29th. On March 31st the first death due to the pandemic was recorded in the State.

Campina Grande is the second largest city in the State of Paraíba. The social distancing policy was implanted in this city on March 20th of 2020, with the closure of universities, schools, and non-essential stores. The social distancing was implemented in a preventive form since the first case of infection by the SARS-CoV-2 virus only came to be registered one week afterwards, on March 27th. The first death due to COVID-19 in this city was only registered on April 19th.

In this work, we adapted the simple and well-known SIR epidemiological model, developed by Kermack and Mckendrick in 1927 [4], to study the evolution of the dissemination of COVID-19. The SIR model is a well-known and tested epidemiological compartmental model that has been applied to very diverse epidemics (see for example Refs. [5–8]). The model receives its name for dividing the population in three groups: susceptible, infected, and removed. Although, SIR and SIR-like models, such as the SIRD and SEIR(D), are simple models compared with far more detailed alternatives, such as proposed by Ndairu *et al.* [9], their simplicity is a strength when it comes to parameter estimation. More complex models have more parameters to be determined, and hence more uncertainties that may render them non viable for large scale applications to many populations. Usually, the available epidemiological data is not complete enough to provide estimates for all the parameters of more complex models. The model we propose here has three independent parameters that need to be estimated from the epidemiological data: contagion rate, average time duration of infection, and lethality rate. We validated the proposed theoretical model with comparisons of official data of the numbers of confirmed, recovered, death, and active cases due to COVID-19 infections in Germany, Brazil, the Brazilian State of Paraíba, and the City of Campina Grande, located in Paraíba. We used a compartmental model called SIRD, which replaces the removed by the recovered and the deceased cases. Furthermore, in the present work we use a time-dependent contagion rate and time-dependent lethality and recovery rates.

SIR(D) or SEIR(D) models with time-dependent contagion rates are not new [10], even for the COVID-19 pandemic there are already several SIR and SIR-like models with time-dependent parameters. The most difficult part of this approach is the design of a parameter estimation method that is automated and renders the model accurate. The early work by Fang *et al.* [11] used a SEIR model in which they estimated the parameters based on the epidemiological data using statistical methods, but at the time of publication there were only about 40 data points and scant comparison of data with theoretical model time series. Zhong *et al.* [12] used a time-dependent SIR model in which they estimate the parameters from the data of active and recovered cases. The authors obtained big fluctuations in the contagion rate and in the removal rate ($1/\tau$). This likely occurred because they approximated the time derivative of the infected (dI/dt) on a daily basis and also, perhaps, because recovered cases data is often less reliable than the confirmed cases data. Chen *et al.* [13] also used a parameter estimation technique of the contagion and the removal rates, but they did not provide information on the parameters obtained in their results explicitly. Dehning *et al.* [14] estimated parameters based on a Bayesian inference with the Markov chain Monte Carlo technique, but not many data points were available at the time of publication and no estimates for

active cases were provided. Linka *et al.* [15] also used a Bayesian parameter estimate in a SEIR model. None of the above articles provide information on estimates for death cases. A comparison of models (SIR, SEIR, and a branching point process) highlighting the strengths and difficulties of each model, and stressing the importance of nonpharmaceutical public health interventions was made by Bertozzi *et al.* [16].

The present work is new in the way it estimates the parameters of the epidemiological model dynamical system. In addition to the adapted SIR model used, we develop a probabilistic model to obtain the recovery and the lethality probabilities. Based on this model, we make estimates for the active cases. The best fit for the active cases provides us with the average time duration of infection, which is held fixed in our model. With the help of this probabilistic model and the epidemiological data, we also obtain the time-dependent parameters of the model: contagion, recovery, and lethality rates. The estimate of the time-dependent contagion rate is based on a fairly simple statistical analysis of the statistical estimate of the active cases. We estimate the time-dependent lethality and recovery rates based on a statistical analysis of the real death cases data. In this way, one avoids the time-consuming task, for the programmer, of obtaining the contagion rate function that leads to the best fit of the data. In this work, the best fit of the data is done automatically in one pass of integration. Thus, this greatly reduces the time taken to fit the available data with the theoretical curve. This also allows for short-time forecasting from one to two weeks in advance. Furthermore, we present and validate a forecasting method based on Markov chains and on the parameter estimation method we use to make short-term predictions of the evolution of the epidemiological variables.

Additionally, we prove the well posedness of this model (existence, unicity, and continuous dependence on initial data). Also, an important theoretical issue we investigate is the dependence of the solutions on the parameters present in the model. As far as we know, this has not been proved yet for this type of model. Hence, we prove the continuous dependence of the solutions on the system parameters. We use techniques similar to those used in [17] and [18] to accomplish this result.

We hope that this study of epidemiological dynamics be useful in stressing the importance of public health policies about the application, maintenance, and reinforcement of social distancing measures with the objective of avoiding the collapse of the health system.

We point out that an earlier version of this work was pre-published in ResearchGate [19].

This work is organized in the following way: In Section II, we propose our epidemiological model and we prove results on existence and uniqueness of solution and on the continuous depen-

dence of the solution with respect to the initial data and the parameters present in the model. We also develop the probabilistic model with estimates of the probabilities of recovery and death. We also describe how to make statistical estimates for the various parameters used in our epidemiological model. In Section III, we investigate the evolution of COVID-19 in Germany as a benchmark test for our model. Afterwards, we present our results and discuss about the evolution of the disease in Brazil, in the State of Paraíba, and in the City of Campina Grande. We validate the predictions of our theoretical model by fitting the official data. Finally, in Section IV we draw our conclusions.

II. EPIDEMIOLOGICAL MODEL

The evolution of the epidemiological model we propose is determined by the following ordinary differential equations (ODE) system

$$\begin{aligned}
 \frac{dS}{dt} &= \nu(S + I + R) - \mu S - \kappa(t)SI, \\
 \frac{dI}{dt} &= -\left(\mu + \frac{1}{\tau}\right)I + \kappa(t)SI, \\
 \frac{dR}{dt} &= \rho(t)I - \mu R, \\
 \frac{dM}{dt} &= \lambda(t)I,
 \end{aligned} \tag{1}$$

where $S(t)$, $I(t)$, $R(t)$ are, respectively, the normalized susceptible, infected, and recovered populations at time t . We define $M(t)$ as the normalized number of accumulated deaths due to the epidemic. The introduction of $M(t)$ is mostly for convenience, so that we do not have to perform a separate integration from the numerical routine used to integrate the differential equations of our model. The normalization of the variables was achieved by dividing them by P_0 , the total initial population of the region considered. For the sake of simplification, we assume that the population is homogeneous such that all the susceptible individuals have the same probability of being contaminated and the infected individuals have the same probability of recovery or death due to the infection. We also suppose that the population evolves in such a way that the newborn babies are all susceptible and the recovered are all immune. The parameter ν is the population birth rate, μ is the death rate before the onset of the pandemic, $\kappa(t)$ is the contagion rate function, $\rho(t)$ is the recovery rate, and $\lambda(t)$ is the lethality rate due to the epidemic. Although $\rho(t)$ and $\lambda(t)$ are changing over time, $\tau^{-1} = \rho(t) + \lambda(t)$ is held constant.

It is important to point out further differences between the original model (1) and the proposed SIR model [4]. This could become relevant if the pandemic lasts for over a year. This is

relevant also as a source of comparison with the death rates due to the COVID-19. One important difference we introduced is that we now allow for time variation in the contagion rate $\kappa(t)$, which reflects changes in confinement, social distancing, and mask use adopted by the population. In addition, we allow for time variation in the recovered and lethality rates, which might reflect possible improvements in the treatment efficacy of COVID-19 and/or changes in the demographics of the infected. Here, we also allow variations in the total population, taking into account the contributions of birth and death rates to the population evolution.

A. Well posedness

In this subsection we prove that, for a given time $T > 0$, for each initial value (S_0, I_0, R_0, M_0) , with $\kappa(t)$, $\rho(t)$ and $\lambda(t)$ varying continuously in the bounded interval $[0, T]$ and with the other parameters fixed, one can show that the ODE system of Eq. (1) admits existence and uniqueness of solution in the time interval $[0, T]$. Furthermore, we prove that the solutions are continuously dependent on the initial data and on the parameters κ , ρ and λ .

To prove the existence and uniqueness of solution of Eq. (1), in the Euclidean space \mathbb{R}^4 , it is sufficient to verify that the function given by the right hand side of Eq. (1) is Lipschitz continuous with respect to spatial variable (see [20]).

For this, let $\xi(t) = (S(t), I(t), R(t), M(t))$ be and define $g : \mathbb{R} \times \mathbb{R}^4 \rightarrow \mathbb{R}^4$ as

$$g(t, \xi) = (g_1(t, \xi), g_2(t, \xi), g_3(t, \xi), g_4(t, \xi)), \quad (2)$$

where the $g_j : \mathbb{R} \times \mathbb{R}^4 \rightarrow \mathbb{R}$ are the coordinate functions of g given by

$$g_1(t, \xi) = \nu(S + I + R) - \mu S - \kappa(t)SI,$$

$$g_2(t, \xi) = - \left(\mu + \frac{1}{\tau} \right) I + \kappa(t)SI,$$

$$g_3(t, \xi) = \rho(t)I - \mu R,$$

and

$$g_4(t, \xi) = \lambda(t)I,$$

with $\kappa, \rho, \lambda : [0, T] \rightarrow \mathbb{R}_+$ continuous functions.

Proposition II.1. *The function given in (2) is Lipschitz continuous with respect to the second variable.*

Proof. Initially we will denote

$$\kappa_{max} = \sup_{t \in [0, T]} \kappa(t) \text{ and } \rho_{max} = \sup_{t \in [0, T]} \rho(t)$$

and we will consider \mathbb{R}^4 with the sum norm, that is, for $\xi = (S, I, R, M)$,

$$\|\xi\| = |S| + |I| + |R| + |M|,$$

where $|S| \leq S_{max}$, $|I| \leq I_{max}$, $|R| \leq R_{max}$ and $|M| \leq M_{max}$.

Hence, it is easy to see that

$$\begin{aligned} |g_1(t, \xi_1) - g_1(t, \xi_2)| &\leq |\nu - \mu||S_1 - S_2| + \nu|I_1 - I_2| + \nu|R_1 - R_2| + \kappa(t)|S_1I_1 - S_2I_2| \\ &\leq |\nu - \mu||S_1 - S_2| + \nu|I_1 - I_2| + \nu|R_1 - R_2| + \kappa(t)|S_1||I_1 - I_2| \\ &\quad + \kappa(t)|I_2||S_2 - S_1| \\ &\leq |\nu - \mu||S_1 - S_2| + \nu|I_1 - I_2| + \nu|R_1 - R_2| + \kappa_{max}S_{max}|I_1 - I_2| \\ &\quad + \kappa_{max}I_{max}|S_1 - S_2| \\ &\leq (|\nu - \mu| + \kappa_{max}I_{max})|S_1 - S_2| + (\nu + \kappa_{max}S_{max})|I_1 - I_2| \\ &\quad + \nu|R_1 - R_2|. \end{aligned}$$

Hence, by writing $L_1 = \sup\{|\nu - \mu| + \kappa_{max}I_{max}, \nu + \kappa_{max}S_{max}\}$, we obtain

$$\begin{aligned} |g_1(t, \xi) - g_1(t, \xi)| &\leq L_1 (|S_1 - S_2| + |I_1 - I_2| + |R_1 - R_2|) \\ &\leq L_1 \|(\xi) - (\xi_2)\|. \end{aligned}$$

Similarly

$$\begin{aligned} |g_2(t, \xi_1) - g_2(t, \xi_2)| &\leq \left(\mu + \frac{1}{\tau}\right) |I_2 - I_1| + \kappa(t)|S_1I_1 - S_2I_2| \\ &\leq \left(\mu + \frac{1}{\tau}\right) |I_2 - I_1| + \kappa(t)|S_1||I_2 - I_1| + \kappa(t)|I_2||S_1 - S_2| \\ &\leq \kappa_{max}I_{max}|S_1 - S_2| + \kappa_{max}S_{max}|I_1 - I_2| + \left(\mu + \frac{1}{\tau}\right)|I_2 - I_1|; \end{aligned}$$

thus, writing $L_2 = \max\{\kappa_{max}I_{max}, \kappa_{max}S_{max} + \mu + \frac{1}{\tau}\}$ we have

$$\begin{aligned} |g_2(t, \xi_1) - g_2(t, \xi_2)| &\leq L_2 (|S_1 - S_2| + |I_1 - I_2|) \\ &\leq L_2 \|(\xi_1) - (\xi_2)\|; \end{aligned}$$

$$\begin{aligned} |g_3(t, \xi_1) - g_3(t, \xi_2)| &\leq \rho(t)|I_1 - I_2| + \mu|R_2 - R_1| \\ &\leq \rho_{max}|I_1 - I_2| + \mu|R_1 - R_2| \\ &\leq L_3 (|I_1 - I_2| + |R_1 - R_2|) \\ &\leq L_3 \|(\xi_2) - (\xi_2)\|, \end{aligned}$$

where $L_3 = \max\{\rho_{max}, \mu\}$, and,

$$|g_4(t, \xi_1) - g_4(t, \xi_2)| \leq \lambda(t)|I_1 - I_2|.$$

Since $\frac{1}{\tau} = \rho(t) + \lambda(t)$, it follows that $\lambda(t) = \frac{1}{\tau} - \rho(t)$. Thus

$$\lambda_{max} = \sup_{t \in [0, T]} \left(\frac{1}{\tau} - \rho(t) \right) < \tau^{-1}.$$

Hence

$$|g_4(t, \xi_1) - g_4(t, \xi_2)| \leq \frac{1}{\tau}|I_1 - I_2| \leq \frac{1}{\tau}\|\xi_1 - \xi_2\|.$$

Therefore,

$$\|g(t, \xi_1) - g(t, \xi_2)\| \leq L\|\xi_1 - \xi_2\|,$$

where $L = \max\{L_1, L_2, L_3, \frac{1}{\tau}\}$. This concludes the proof.

Remark II.2. From Proposition II.1 and Picard-Lindelöf Theorem [20], it follows that for each initial value $\xi_0 = (S_0, I_0, R_0, M_0)$, with $\kappa(t)$, $\rho(t)$ and $\lambda(t)$ varying continuously in the bounded intervals $[0, T]$, the ODE system of Eq. (1) admits existence and uniqueness of solution in the time interval $[0, T]$, which is given, for $t \in [0, T]$, by

$$\xi(t) = \xi_0 + \int_0^t g(s, \xi(s)) ds. \quad (3)$$

Furthermore, using (3) and Gronwall inequality [20], we obtain the sensitivity with respect to the initial data.

Indeed, denoting by $\xi(t, \xi_0)$ the solution of Eq. (1) that at $t = 0$ is ξ_0 , we have

$$\begin{aligned} \|\xi(t, \xi_0^1) - \xi(t, \xi_0^2)\| &\leq \|\xi_0^1 - \xi_0^2\| + \int_0^t \|g(s, \xi(s, \xi_0^1)) - g(s, \xi(s, \xi_0^2))\| ds \\ &\leq \|\xi_0^1 - \xi_0^2\| + \int_0^t L\|\xi(s, \xi_0^1) - \xi(s, \xi_0^2)\| ds. \end{aligned}$$

Hence, from Gronwall inequality

$$\begin{aligned} \|\xi(t, \xi_0^1) - \xi(t, \xi_0^2)\| &\leq \|\xi_0^1 - \xi_0^2\| e^{\int_0^t L ds} \\ &\leq e^T \|\xi_0^1 - \xi_0^2\| \rightarrow 0, \text{ as } \|\xi_0^1 - \xi_0^2\| \rightarrow 0. \end{aligned}$$

B. Continuous dependence on parameters

In this subsection we investigate the continuous dependence of the solutions of (1) with respect to the variation of its main parameters

Proposition II.3. *Under the same assumptions and notation from Proposition II.1, the solution $(S(t), I(t), R(t), M(t))$ is continuous with respect to parameters $\kappa(t)$, $\rho(t)$ and $\lambda(t)$ present in Eq. (1).*

Proof. Define $\theta : [0, T] \rightarrow \mathbb{R}^3$ by

$$\theta(t) = (\kappa(t), \rho(t), \lambda(t)).$$

Consider the metric defined on space of the continuous functions of $[0, T]$ in \mathbb{R}^3 , $\mathbb{C}([0, T], \mathbb{R}^3)$, given by

$$\text{dist}(\theta, \theta_0) = \sup_{t \in [0, T]} |\kappa(t) - \kappa_0(t)| + \sup_{t \in [0, T]} |\rho(t) - \rho_0(t)| + \sup_{t \in [0, T]} |\lambda(t) - \lambda_0(t)|.$$

Now, we denote by $\xi_\theta(t)$ the solutions of Eq. (1) with respect to parameter $\theta(t) = (\kappa(t), \rho(t), \lambda(t))$ such that $\xi_\theta(0) = \xi_0$ and we denote by $\xi_{\theta_0}(t)$ the solutions with respect to parameter $\theta_0(t) = (\kappa_0(t), \rho_0(t), \lambda_0(t))$ such that $\xi_{\theta_0}(0) = \xi_0$.

We need to show that

$$\|\xi_\theta(t) - \xi_{\theta_0}(t)\| \rightarrow 0, \text{ as } \text{dist}(\theta, \theta_0) \rightarrow 0.$$

For this, note that

$$\|\xi_\theta(t) - \xi_{\theta_0}(t)\| \leq \int_0^t \|g(s, \xi_\theta(s)) - g(s, \xi_{\theta_0}(s))\| ds. \quad (4)$$

Now

$$\begin{aligned} |g_1(s, \xi_\theta(s)) - g_1(s, \xi_{\theta_0}(s))| &= |\nu[S(s) - S_0(s)] + \nu[I(s) - I_0(s)] + \nu[R(s) - R_0(s)] \\ &\quad + \mu[S_0(s) - S(s)] + \kappa(s)S(s)I(s) - \kappa_0(s)S_0(s)I_0(s)| \\ &\leq (\nu + \mu)|S(s) - S_0(s)| + \nu|I(s) - I_0(s)| + \nu|R(s) - R_0(s)| \\ &\quad + |\kappa(s)S(s)I(s) - \kappa_0(s)S(s)I(s)| \\ &\quad + |\kappa_0(s)S(s)I(s) - \kappa_0(s)S_0(s)I_0(s)|. \end{aligned}$$

But

$$|\kappa(s)S(s)I(s) - \kappa_0(s)S(s)I(s)| = |S(s)I(s)||\kappa(s) - \kappa_0(s)|$$

and

$$\begin{aligned} |\kappa_0(s)S(s)I(s) - \kappa_0(s)S_0(s)I_0(s)| &= |\kappa_0(s)|S(s)I(s) - S_0(s)I_0(s)| \\ &\leq \kappa_0(s) (|S(s)||I(s) - I_0(s)| + |I_0(s)||S(s) - S_0(s)|). \end{aligned}$$

Hence

$$\begin{aligned}
|g_1(s, \xi_\theta(s)) - g_1(s, \xi_{\theta_0}(s))| &\leq (\nu + \mu)|S(s) - S_0(s)| + \nu|I(s) - I_0(s)| + \nu|R(s) - R_0(s)| \\
&\quad + S_{max} I_{max} \sup_{s \in [0, T]} |\kappa(s) - \kappa_0(s)| \\
&\quad + \kappa_{0max} (S_{max} |I(s) - I_0(s)| + I_{0max} |S(s) - S_0(s)|) \\
&\leq (\nu + \mu + \kappa_{0max} I_{0max})|S(s) - S_0(s)| \\
&\quad + (\nu + \kappa_{0max} S_{max})|I(s) - I_0(s)| + \nu|R(s) - R_0(s)| \\
&\quad + S_{max} I_{max} dist(\theta, \theta_0).
\end{aligned}$$

Thus, by writing $G_1 = \{\nu + \mu + \kappa_{0max} I_{0max}, \nu + \kappa_{0max} S_{max}\}$, we obtain

$$|g_1(s, \xi_\theta(s)) - g_1(s, \xi_{\theta_0}(s))| \leq G_1 \|\xi_\theta(s) - \xi_{\theta_0}(s)\| + S_{max} I_{max} dist(\theta, \theta_0). \quad (5)$$

$$\begin{aligned}
|g_2(s, \xi_\theta(s)) - g_2(s, \xi_{\theta_0}(s))| &= \left| \left(\mu + \frac{1}{\tau} \right) (I_0 - I) + \kappa(s)S(s)I(s) - \kappa_0(s)S_0(s)I_0(s) \right| \\
&\leq \left(\mu + \frac{1}{\tau} \right) |I_0 - I| + |S(s)I(s)| |\kappa(s) - \kappa_0(s)| \\
&\quad + |\kappa_0(s)| |S(s)I(s) - S_0(s)I_0(s)| \\
&\leq \left(\mu + \frac{1}{\tau} \right) |I_0 - I| + S_{max} I_{max} |\kappa(s) - \kappa_0(s)| \\
&\quad + \kappa_{0max} (|S(s)| |I(s) - I_0(s)| + |I_0(s)| |S(s) - S_0(s)|) \\
&\leq \kappa_{0max} I_{0max} |S(s) - S_0(s)| + \left(\mu + \frac{1}{\tau} + \kappa_{0max} S_{max} \right) |I_0 - I| \\
&\quad + S_{max} I_{max} dist(\theta, \theta_0) \\
&\leq G_2 \|\xi_\theta - \xi_{\theta_0}\| + S_{max} I_{max} dist(\theta, \theta_0), \quad (6)
\end{aligned}$$

where $G_2 = \max\{\kappa_{0max} I_{0max}, \mu + \frac{1}{\tau} + \kappa_{0max} S_{max}\}$.

$$\begin{aligned}
|g_3(s, \xi_\theta(s)) - g_3(s, \xi_{\theta_0}(s))| &= |\rho(s)I(s) - \rho_0(s)I_0(s) + \mu[R_0(s) - R(s)]| \\
&\leq |I(s)| |\rho(s) - \rho_0(s)| + |\rho_0(s)| |I(s) - I_0(s)| \\
&\quad + \mu |R_0(s) - R(s)| \\
&\leq I_{max} \sup_{s \in [0, T]} |\rho(s) - \rho_0(s)| + \left(\sup_{s \in [0, T]} \rho_0(s) \right) |I(s) - I_0(s)| \\
&\quad + \mu |R_0(s) - R(s)| \\
&\leq I_{max} dist(\theta, \theta_0) + \rho_{0max} |I(s) - I_0(s)| \\
&\quad + \mu |R_0(s) - R(s)| \\
&\leq G_3 \|\xi_\theta(s) - \xi_{\theta_0}(s)\| + I_{max} dist(\theta, \theta_0),
\end{aligned}$$

where $G_3 = \max\{\rho_{0max}, \mu\}$. Now,

$$\begin{aligned} |g_4(s, \xi_\theta(s)) - g_4(s, \xi_{\theta_0}(s))| &= |\lambda(s)I(s) - \lambda_0(s)I_0(s)| \\ &\leq |I(s)||\lambda(s) - \lambda_0(s)| + \lambda_0(s)|I(s) - I_0(s)| \\ &\leq I_{max} \left(\sup_{s \in [0, T]} |\lambda(s) - \lambda_0(s)| \right) + \left(\frac{1}{\tau} - \rho_0(s) \right) |I(s) - I_0(s)| \\ &\leq \frac{1}{\tau} \|\xi_\theta(s) - \xi_{\theta_0}(s)\| + I_{max} \text{dist}(\theta, \theta_0). \end{aligned}$$

Thus, by using (5), (6), (7) and (7) in (4), we have

$$\begin{aligned} \|\xi_\theta(t) - \xi_{\theta_0}(t)\| &\leq \int_0^t \{2(S_{max}I_{max} + I_{max})\text{dist}(\theta, \theta_0) + (G_1 + G_2 + G_3 + \frac{1}{\tau})\|\xi_\theta(s) - \xi_{\theta_0}(s)\|\} ds \\ &\leq 2T(S_{max}I_{max} + I_{max})\text{dist}(\theta, \theta_0) + \int_0^t \left(G_1 + G_2 + G_3 + \frac{1}{\tau} \right) \|\xi_\theta(s) - \xi_{\theta_0}(s)\| ds. \end{aligned}$$

Therefore, from Gronwall Lemma, it follows that

$$\|\xi_\theta(t) - \xi_{\theta_0}(t)\| \leq 2T(S_{max}I_{max} + I_{max})\text{dist}(\theta, \theta_0)e^{(G_1+G_2+G_3+\frac{1}{\tau})T} \rightarrow 0,$$

as $\text{dist}(\theta, \theta_0)$.

III. ESTIMATES FOR THE PARAMETERS

In this section, we explain some estimates for the parameters present in the model.

A. Reproduction number

It is of paramount importance to know if a contagious disease will become epidemic or not in a population. It is also important to know when it will be possible to control an epidemic, that is, when it will be possible to block its growth. This will happen when $\frac{dI}{dt} \leq 0$. From Eq. (1), we verify that this condition is equivalent to

$$-\left(\mu + \frac{1}{\tau}\right) + \kappa S(t) \leq 0 \implies \frac{\kappa S(t)}{\mu + \frac{1}{\tau}} \leq 1. \quad (7)$$

In the beginning of the epidemic we obtain that the value of the following ratio

$$R_0 = \frac{\kappa S_0}{\mu + 1/\tau},$$

known in the literature [21] as the basic reproduction number, is what indicates whether we will have an epidemic or not. When $R_0 > 1$, the disease will spread, whereas when $R_0 < 1$ the

contagion loses strength and the dissemination of the virus will be controlled. In our case $S_0 = 1$ and $S(t) \leq 1$, thus at any time after the onset of the epidemic the disease will stop spreading when

$$R_0(t) = \frac{\kappa(t)S(t)}{\mu + 1/\tau} \leq 1. \quad (8)$$

We have that $R_0 < 1$ is a sufficient condition that the epidemic will enter remission, but in general it is not a necessary condition. The necessary condition is that $R_0(t) < 1$. Although, we are just over 5 months into the current epidemic in Brazil at the time of writing, $M(t) \ll 1$, $S(t) \approx 1$, the critical condition is still approximately $R_0 = 1$ and the critical value of $\kappa(t)$ is $\kappa^* = \mu + 1/\tau$.

As there is no efficacious treatment against COVID-19 at the time of writing this paper to the authors' knowledge, it is not yet possible to easily alter the average time of infection τ . As $1/\tau \gg \mu$, thus the only viable manner of decreasing $R_0(t) \approx \kappa(t)\tau$ is by reducing the value of $\kappa(t)$, which can be obtained with social distancing measures and the use of PPEs.

B. Probabilistic model

It is fundamental that we have good estimates for the recovery and the lethality rates. In order to obtain these estimates we will use a very simple probabilistic model. Suppose that a person is infected at a given instant n (which may be a day, an hour, or a minute for example), then the probability that the infected remains sick until the following instant $n + 1$ is q , the probability that the infected recovers in the next instant is p , and the probability that the infected dies is s , in such a way that $p + q + s = 1$. Here, we suppose that q and $p + s$ remain constant during the course of the disease. Hence, we have the following probability table

TABLE I. Probabilistic model

Situation \ Instant	0	1	2	...	n	...
Recovered	p	qp	q^2p	...	$q^n p$...
Death	s	qs	q^2s	...	$q^n s$...

Note that the normalization

$$\sum_{n=0}^{\infty} q^n p + \sum_{n=0}^{\infty} q^n s = \frac{p + s}{1 - q} = 1,$$

implies that this probabilistic model is well defined.

If n is sufficiently large, only two outcomes are possible: either the infected individual recovers or dies. Hence, based on the Table I we find that the probability of recovery and of death

are, respectively,

$$\begin{aligned} P_\rho &= \sum_{n=0}^{\infty} pq^n = p/(1-q), \\ P_\lambda &= \sum_{n=0}^{\infty} sq^n = s/(1-q). \end{aligned} \quad (9)$$

Using these probabilities we find that the average number of instants (minutes, hours, days, etc) of the infection is given by

$$\bar{n} = \sum_{n=1}^{\infty} (p+s)nq^n = (p+s)F_1(q) = (1-q) \sum_{n=1}^{\infty} nq^n, \quad (10)$$

in which the summation $F_1(q) = \sum_{n=1}^{\infty} nq^n$ can be calculated in the following form

$$qF_1(q) = \sum_{n=1}^{\infty} nq^{n+1} = \sum_{n=2}^{\infty} (n-1)q^n = \sum_{n=2}^{\infty} nq^n - \sum_{n=2}^{\infty} q^n = F_1(q) - \sum_{n=1}^{\infty} q^n = F_1(q) - \frac{q}{1-q}.$$

Hence, we obtain

$$F_1(q) = \frac{q}{(1-q)^2}. \quad (11)$$

Therefore, we find that the average number of instants of the infection is

$$\bar{n} = \frac{q}{1-q}, \quad (12)$$

from where we obtain that $q = \bar{n}/(1 + \bar{n})$. We can also find that the average number of time intervals until recovery is given by

$$\bar{n}_\rho = pF_1(q) = \frac{pq}{(1-q)^2} = P_\rho \bar{n}$$

and the average number of time intervals until death is

$$\bar{n}_\lambda = sF_1(q) = \frac{sq}{(1-q)^2} = P_\lambda \bar{n}.$$

Note that $\bar{n} = \bar{n}_\rho + \bar{n}_\lambda$, that is, the average infection time span is the sum of the average time span for recovery and the average time span until death. If only these two processes were present, it would lead to the following difference equation for the number of infected

$$I(n+1) = I(n) - (p+s)I(n) = I(n) - (1-q)I(n) = I(n) - \frac{1}{1+\bar{n}}I(n).$$

If we take n to indicate the n -th time interval, such as a minute, in which there is not much variation in the quantities S , I , R , and M , hence, we can approximate

$$\frac{dI}{dt} \approx \frac{\Delta I}{\Delta t} = -\frac{1}{(1+\bar{n})\Delta t} I(t_n),$$

in which $t_n = n\Delta t$. In this work, we take $\Delta t = 1 \text{ hour} = 1 \text{ day}/24$. The average time span of infection can be obtained from the following equation

$$\frac{1}{\tau} = \lambda + \rho = \frac{1}{(1 + \bar{n})\Delta t}. \quad (13)$$

Hence, we obtain the following expressions for the rates of lethality and recovery

$$\begin{aligned} \lambda &= \frac{\bar{n}_\lambda}{\bar{n}\tau} = \frac{P_\lambda}{\tau}, \\ \rho &= \frac{\bar{n}_\rho}{\bar{n}\tau} = \frac{P_\rho}{\tau}. \end{aligned} \quad (14)$$

1. Standard deviation

Here, we calculate the standard deviation for this probabilistic process in the number of time intervals n of infection, from the contamination until recovery or death. In order to achieve that, we have first to calculate the sum

$$F_2(q) = \sum_{n=1}^{\infty} n^2 q^n. \quad (15)$$

We can calculate this sum by noting that

$$q^2 F_2(q) = \sum_{n=2}^{\infty} (n-2)^2 q^n = F_2(q) + 4 \sum_{n=1}^{\infty} (1-n)q^n = F_2(q) + \frac{4q}{1-q} - q - 4F_1(q).$$

Hence, we find

$$F_2(q) = \frac{q(1+q)}{(1-q)^3}. \quad (16)$$

We then obtain

$$\overline{n^2} = (1-q)F_2(q) = \frac{q(1+q)}{(1-q)^2}$$

and

$$\bar{n}^2 = \frac{q^2}{(1-q)^2}.$$

We can now write the standard deviation of n as

$$\sigma = \sqrt{\overline{n^2} - \bar{n}^2} = \frac{\sqrt{q}}{1-q}. \quad (17)$$

This shows that the statistical fluctuations in the time duration of the infection as q grows to 1. By reducing q one not only decreases \bar{n} but also σ .

C. Statistical prediction of active, recovery, and death cases

It is very important for government officials to have estimates of the number of active (infected) cases in a given population, since these people are the ones who spread the disease. Based on knowledge of new daily infections (new confirmed cases), which we can obtain from COVID-19 databases that are updated at least every day with data from across the globe, we can make several estimates. One simple estimate of the number of active cases at time t_k is

$$A(t_k) = C(t_k) - \mathcal{R}(t_k) - D(t_k) \approx C(t_k) - C(t_k - \tau), \quad (18)$$

where $C(t_k)$ is the number confirmed cases, $\mathcal{R}(t_k)$ is the number of recovered cases, $D(t_k)$ represents the accumulated number of death cases at time t_k . Another approach is to make a statistical estimate for the number of active cases at time t_k that follows the probabilistic process described in Sec. III B, which is the following

$$A(t_k) = - \sum_{i=-1}^k q^i P_0 \Delta S(t_{k-i}) = \sum_{i=0}^k q^i \Delta C(t_{k-i}), \quad (19)$$

where $A(t_k) = P_0 I(t_k)$, $\Delta S(t_n) = S(t_n) - S(t_{n-1})$ and, likewise, $\Delta C(t_n) = C(t_n) - C(t_{n-1})$. The index k starts at 0. We also have the following probabilistic estimates for the daily increase of recovered and death cases at the k -th day

$$\Delta \mathcal{R}(t_k) = \sum_{i=0}^{k-1} q^i p \Delta C(t_{k-1-i}), \quad (20)$$

$$\Delta D(t_k) = \sum_{i=0}^{k-1} q^i s \Delta C(t_{k-1-i}), \quad (21)$$

These probabilistic estimates complement the predictions from the epidemiological dynamical system model. The probabilistic aspect of the pandemic evolution can be most clearly seen when one considers short time variations, such as daily data on the number of new confirmed, recovered, or death cases. Also this allows us to make estimates of the evolution of the active, recovered, and death cases solely from the confirmed cases time series. This is most important where the recovered cases are not available or are less reliable, specially when one is counting the recovery of outpatients, since they may not take a second test to show they are actually free of the infection.

D. Estimates of the parameters used in the model

We now make some estimates for the parameters ν , μ , ρ , and λ present in the dynamical system given in Eq. (1).

1. Birth and death rates

In order to make our model more precise, we obtained the annual birth rate (ABR) and the annual mortality rate (AMR) from the most recently published data from Germany and from Brazil before the spread of the pandemic.

We also converted these annual rates into daily rates using the geometrical progression formulas

$$(1 + \nu)^{365} = 1 + ABR,$$

$$(1 - \mu)^{365} = 1 - AMR.$$

Hence, we find the daily birth and mortality rates

$$\nu = (1 + ABR)^{1/365} - 1 = e^{\frac{1}{365} \ln(1+ABR)} - 1$$

$$\mu = 1 - (1 - AMR)^{1/365} = 1 - e^{\frac{1}{365} \ln(1-AMR)}$$
(22)

The German data on birth and death rates were obtained from the Federal Statistical Office [22, 23]. The Brazilian data was obtained from the Brazilian Institute of Geography and Statistics (IBGE), which are from 2018. For the birth rate we divided the number of born alive infants by the population estimate for 2018 and, likewise, the number of deaths by the 2018 population estimate. The data on the born alive was collected from the site <https://sidra.ibge.gov.br/tabela/2609>, the number of deaths from the site <https://sidra.ibge.gov.br/tabela/2654>, and the population estimate from the site <https://www.ibge.gov.br/estatisticas/sociais/populacao/9103-estimativas-de-populacao.html?edicao=22367&t=resultados>. The birth and death rates used are shown in the table II below. We provide table III with information on the average total daily deaths (without the born dead) before the pandemic based on annual death rates from 2018. This should be compared with the average daily deaths due to COVID-19 as another way of assessing the severity of this pandemic.

TABLE II. Birth and death rates

Population	ABR (year ⁻¹)	ν (day ⁻¹)	AMR (year ⁻¹)	μ (day ⁻¹)
Germany	0.0095	2.591×10^{-5}	0.0115	3.169×10^{-5}
Brazil	0.0139	3.7844×10^{-5}	6.1560×10^{-3}	1.6918×10^{-5}
Paraíba	0.0148	4.0139×10^{-5}	6.5325×10^{-3}	1.7956×10^{-5}
Campina Grande	0.0158	4.2943×10^{-5}	7.1342×10^{-3}	1.9616×10^{-5}

TABLE III. Pre-pandemic populations and average daily deaths

Location	P_0	$\mu(\text{day}^{-1})$	average deaths (day^{-1})
Germany	83,149,360	3.169×10^{-5}	2635
Brazil	211,049,527	1.6918×10^{-5}	3570
Paraíba	4,018,127	1.7956×10^{-5}	72
Campina Grande	409,731	1.9616×10^{-5}	8

2. Contagion rate

We use the following method to estimate the time-dependent contagion rate. From Eq. (1), we can write

$$\kappa(t) = \frac{1}{S(t)} \left[\frac{1}{I(t)} \frac{dI(t)}{dt} + \mu + \frac{1}{\tau} \right]. \quad (23)$$

This can be approximated by

$$\kappa_k = \kappa(t_k) \approx \frac{1}{S(t_k)} \left[\frac{1}{A(t_k)} \frac{\Delta A(t_k)}{\Delta t} + \mu + \frac{1}{\tau} \right], \quad (24)$$

where $\Delta t = 1\text{day}$. The daily approximation has too much fluctuation. A better approach is to replace the daily derivative by the slope of a linear regression of 7 consecutive active cases data points $\{A_k, A_{k+1}, \dots, A_{k+6}\}$. One rolls this week-long window over the entire set of data points calculating κ_k . For the last six days of data, we use a backwards window with the data points $\{A_k, A_{k-1}, \dots, A_{k-6}\}$. We chose the week interval, because all epidemiological data we have seen present weekly modulations. The most difficult part of this estimating method of $\kappa(t)$ occurs at the beginning of the data sets, when the number of active cases is very small. From Eq. (24), one can see that for small values of $A(t_k)$, any errors in the derivative approximation $\frac{\Delta A(t_k)}{\Delta t}$ are amplified. Therefore, in most cases we discard the first days or weeks of epidemiological data, usually up to the day the first death occurred. In some cases, we also had to apply a cutoff to eliminate the highest values of $\kappa(t)$ right at the beginning of the time series. Apart from the numerical errors described above, notice that any new imported infected case contributes strongly to the spread of the disease near the outbreak of the epidemic. Hence, at the beginning $\kappa(t)$ tends to be very high. This also reflects the fact that at the start of the pandemic most populations did not keep social distancing nor used PPEs such as masks.

3. Lethality and recovery rates

We use the following method to estimate the time-dependent lethality rate. Based on Eq.(21), we can write the probability of dying for those infected with COVID-19 in a one day time interval as

$$s_k = \frac{\Delta D(t_k)}{\sum_{i=0}^{k-1} q^i \Delta C(t_{k-1-i})}. \quad (25)$$

From this we obtain the daily lethality probability $P_\lambda(k)$ from Eq. (9). Afterwards, from Eq. (III B) we find the lethality rate λ_k for the k -th day. Consequently, from $\rho_k + \lambda_k = 1/\tau$ we also find the recovery rate ρ_k at the k -th day. The simpler approach of estimating s_k with $\Delta D_k/A_{k-1}$ introduces far more fluctuations.

E. Forecasting

We use a list with the last three weeks of $\kappa(t)$ data to calculate the transition probabilities of a simple two-state Markov chain as shown in Fig. 1. From this list, we obtain a list of differences $\Delta\kappa_i = \kappa(t_i) - \kappa(t_{i-1})$. Based on this, we make two probability distributions, one for increments in $\kappa(t)$ and the other for decrements. If $\Delta\kappa_i < 0$, in the differences list, we replace it with 0, otherwise we replace it with 1. From this list of 0's and 1's, we obtain a list of lengths of the continuous sequences of 0's and 1's. We then obtain the average length of continuous stretches of 0's and 1's. We call the average length of increments of the contagion rate \bar{n}_+ and of decrements \bar{n}_- . Based on this we find the following transition probabilities

$$\begin{aligned} q_{++} &= \frac{\bar{n}_+}{1 + \bar{n}_+}, & p_{+-} &= 1 - q_{++}, \\ q_{--} &= \frac{\bar{n}_-}{1 + \bar{n}_-}, & p_{-+} &= 1 - q_{--}. \end{aligned} \quad (26)$$

Now we use the Markov chain to decide between increasing or decreasing $\kappa(t)$. The values of the increments or decrements are taken from the two probability distributions obtained as described above. We then randomly obtain predicted values of κ for two weeks based on a three-week history of data. We repeat this process for 1000 times and make an average of all these trajectories as it is depicted in Fig. 5. From these trajectories we also obtain a 95% confidence interval. In the figure, we compare actual data with our predictions for the two most recent weeks. Using this same approach, we can forecast the lethality rate based on a list of daily variation of $\lambda(t)$.

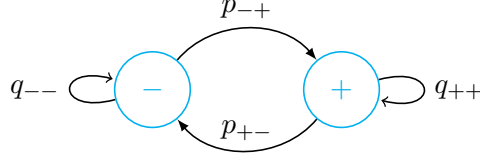


FIG. 1. Markov chain diagram with transition probabilities. In the $-$ state $\kappa(t)$ is decreasing in time, while in the $+$ state, it is increasing.

IV. RESULTS AND DISCUSSION

The data of the number of confirmed, recovered and death cases from Germany and Brazil were obtained from the site <<https://data.humdata.org/dataset/novel-coronavirus-2019-ncov-cases>>, (accessed on 11/01/2020, with data collected until 10/31). We obtained the time series of confirmed and death cases of the State of Paraíba and the City of Campina Grande in the site: https://data.Brazil.io/dataset/covid19/_meta/list.html (accessed on 11/01/2020, with data collected until 10/31).

We used the Odeint function of the Python's scientific library package SciPy [24] to integrate the ODE system of Eq. (1) with the integration time-step $dt = 1.0/24$, which corresponds to an hour when the time unit is a day. In the cases investigated, we took τ 13-14 days. We chose the value that provided the best fit of the active cases with the delay estimate given in Eq. (18) when the active cases data was available, such as in the cases of Germany and Brazil. When the active cases data was not available, we chose τ that would give the best fit between the theoretical prediction for the active cases and the corresponding estimate of Eq. (18). We suppose this parameter does not change appreciably during the time scale of the outbreak of the pandemic until now, or at least until more efficient treatments are discovered. The initial values used are: $S(0) = 1 - C_0/P_0$, $I(0) = A_0/P_0$, $R(0) = \mathcal{R}_0/P_0$, and $M(0) = D_0/P_0$, with P_0 being the population just before the outbreak of the pandemic, C_0 is the initial number of confirmed cases, A_0 is the initial number of active cases, \mathcal{R}_0 is the initial number of recovered cases, and D_0 is the initial number of death cases, usually either 0 or 1. We now apply our model to the four cases of COVID-19 dissemination: in Germany, in Brazil, in the State of Paraíba, and in the City of Campina Grande.

In Fig. 2, we show results of numerical simulation for a range of values of κ . Unlike the other results, κ is held constant during each time integration of the equations of motion given in Eq. (1). This result is important in conveying the message of the paramount importance of the contagion rate on the possible outcomes of the pandemic. Not only we observe an increase in the

number of deaths when the contagion rates increase, but we also see a sharp transition. When there is a growth in the contagion rate from 0.1 to 0.15, this gives rise to an extremely sharp increase in the number of deaths. This implies that there is a critical value of κ , around which there is a rapid increase in the total number of deaths due to the pandemic. Beyond the critical value, we see a saturation in the total number of deaths. The value of κ that corresponds to $R_0 = 1$ in our model is $\kappa = \mu + 1/\tau = 0.0714$. We believe, this reinforces the great relevance of social distancing, since increasing the average distance between people, we will be decreasing the rate of contagion and, consequently, decreasing also the number of deaths due to COVID-19.

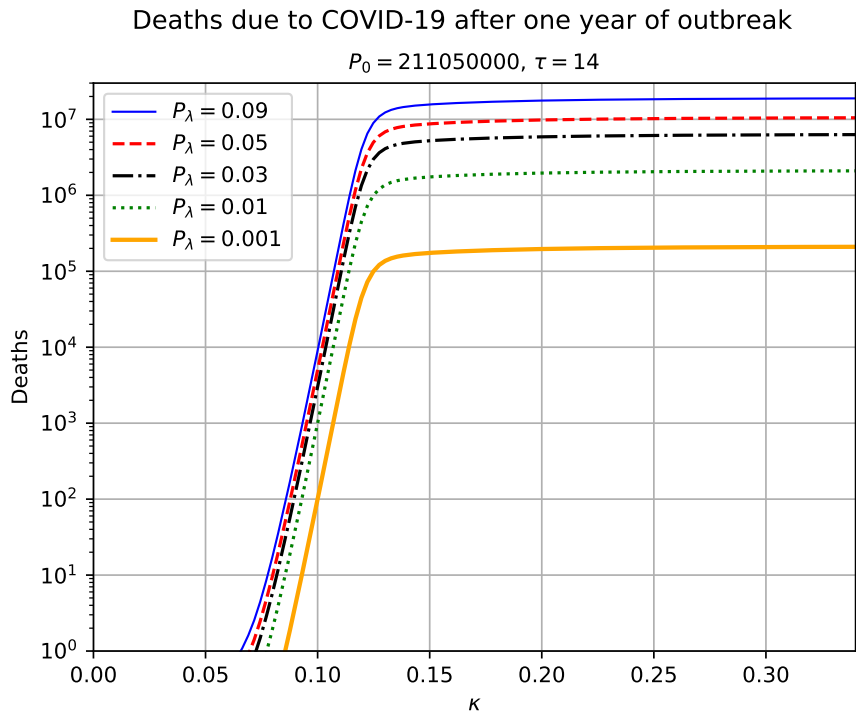


FIG. 2. Total number of accumulated deaths as a consequence of the epidemic as a function of the contagion rate κ . The total time duration for each value of κ is 365 days. The used parameters in this simulation are indicated above the figure. The value of κ that corresponds to $R_0 = 1$ is $\kappa^* = \mu + 1/\tau = 0.0714$.

A. Evolution of COVID-19 in Germany

We consider the case of Germany as a benchmark test for our epidemiological model. This is so because it is widely believed that the cases from Germany are better accounted for than in most other countries, with widespread testing of the population <https://www.labmate-online.com/news/laboratory-products/3/breaking-news/how-germany-ha>

[s-led-the-way-on-covid-19-testing/52141](#). The initial population considered is $P_0 = 83.14936$ millions. The first contagion was registered on 01/27/2020 and the first death due to COVID-19 was registered on 03/09/2020. We chose this latter date as the initial point of our numerical integration.

In Fig. 3A, we show the official data on the confirmed cases of COVID-19 plotted alongside the theoretical prediction, in which a very good agreement with the epidemiological data was obtained. The contagion rate function used is given in Fig. 4. In frame B, we plot the recovered cases data along with the theoretical predictions based on our model. In frame C, we plot the death cases with respective theoretical curve. In frame D, we plot the active cases data along with the theoretical predictions based on our model. The theoretical fit is not as good as in the previous figures, but it is still quite reasonable. We see a slow decline in the number of infected. Once the total number of confirmed cases basically saturates, the evolution of the active cases can be traced with a purely statistical model as the one we developed in Sec. III B. From the statistical point of view the slow decay of the active cases has to do with the large value of the dispersion in the duration of the infection, as shown in Sec. III B 1. We also plot two estimates of the active cases obtained solely from an analysis of the confirmed cases data. The delay estimate of active cases at a given time t is based on Eq. 18. The statistical estimate is obtained from the probabilistic process given in Eq. 19. This estimate came closer to the theoretical dynamical system model, what shows its consistency with the probabilistic model of Sec. III B. Both estimates came fairly close to the real data. In the present case, they seem to bracket the real data. Note also, that at the last two weeks of the time series we validate the forecasting model based on the Markov chain. Here, we show a 95% confidence band along two weeks. In this case the all epidemiological data fell within the predictions.

In Fig. 4A, we show the graph with the parameter estimation for the contagion rate function $\kappa(t)$. At the beginning of the time series, the contagion rate is very high. To achieve the best fit between theory and the data in Fig.(3), we had a cutoff at $\kappa = 0.41$, otherwise we used the estimation method described in Sec. III D 2 to obtain this time series. Note that we observe weekly modulations, likely reflecting the fact that in weekdays the contamination is higher than in weekends. The rapid decrease of $\kappa(t)$ intensifies approximately around 03/22/2020, when strict social distancing rules were imposed by the German Government [14, 25]. This shows that these measures were very efficient in containing the spread of the epidemic. In frame B, we show the corresponding reproduction number time series. Around April/09, the $R_0(t)$ becomes below 1 and stays there until about June/13, when for a period of roughly 10 days it rose slightly above 1. In frame C we

show the time-dependent lethality and recovery rates, $\lambda(t)$ and $\rho(t) = 1/\tau - \lambda(t)$, respectively. These estimates were obtained using the method described in Sec. III D 3.

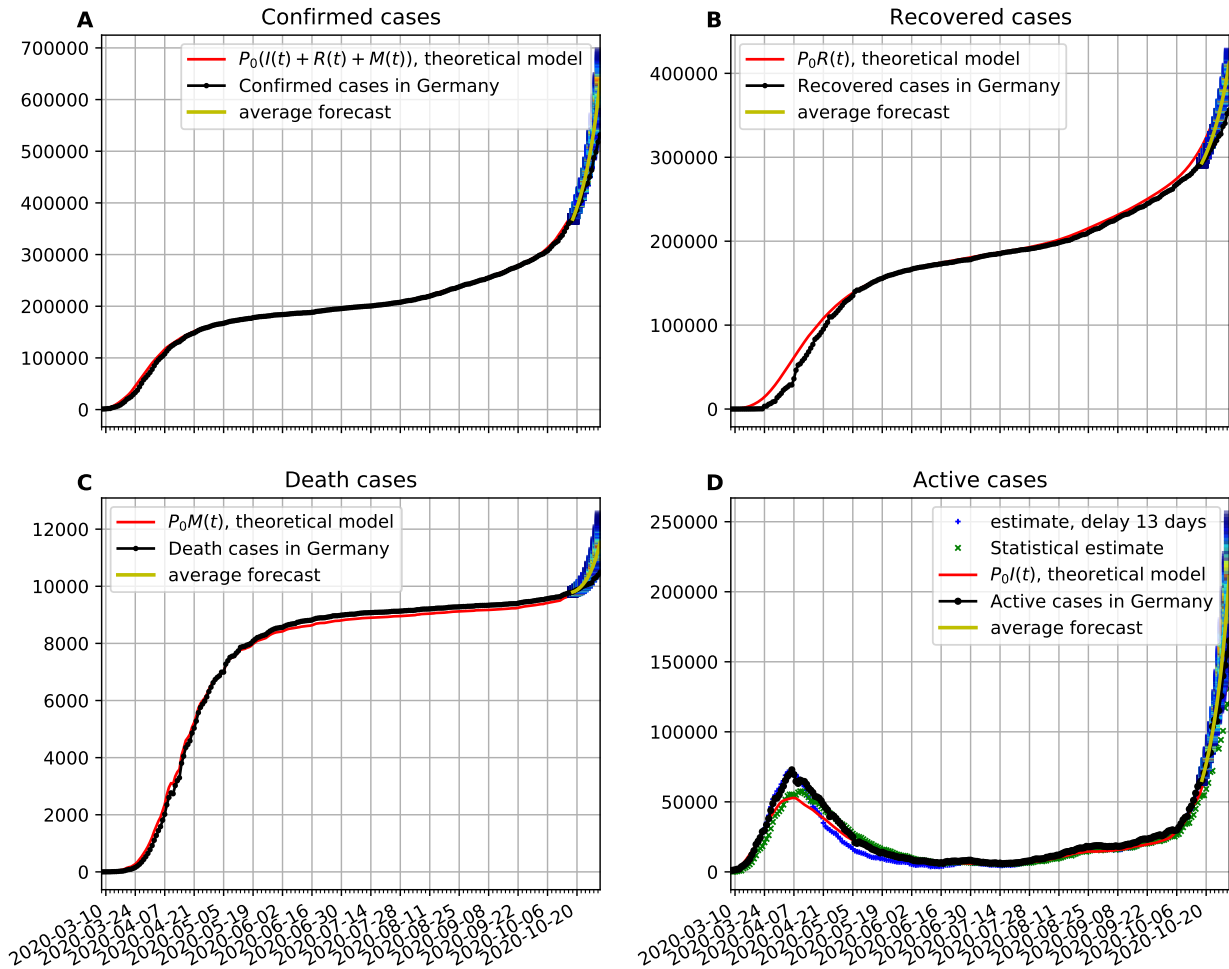


FIG. 3. **A** Confirmed cases data compared with the theoretical prediction. **B** Recovered cases data in comparison with the theoretical prediction. **C** Death cases data compared with the theoretical prediction. **D** Active cases compared with delay estimate, statistical estimate, and the predicted theoretical curve. In all cases the functions $\kappa(t)$, $\lambda(t)$, and $\rho(t)$ vary in time according to Fig. 4.

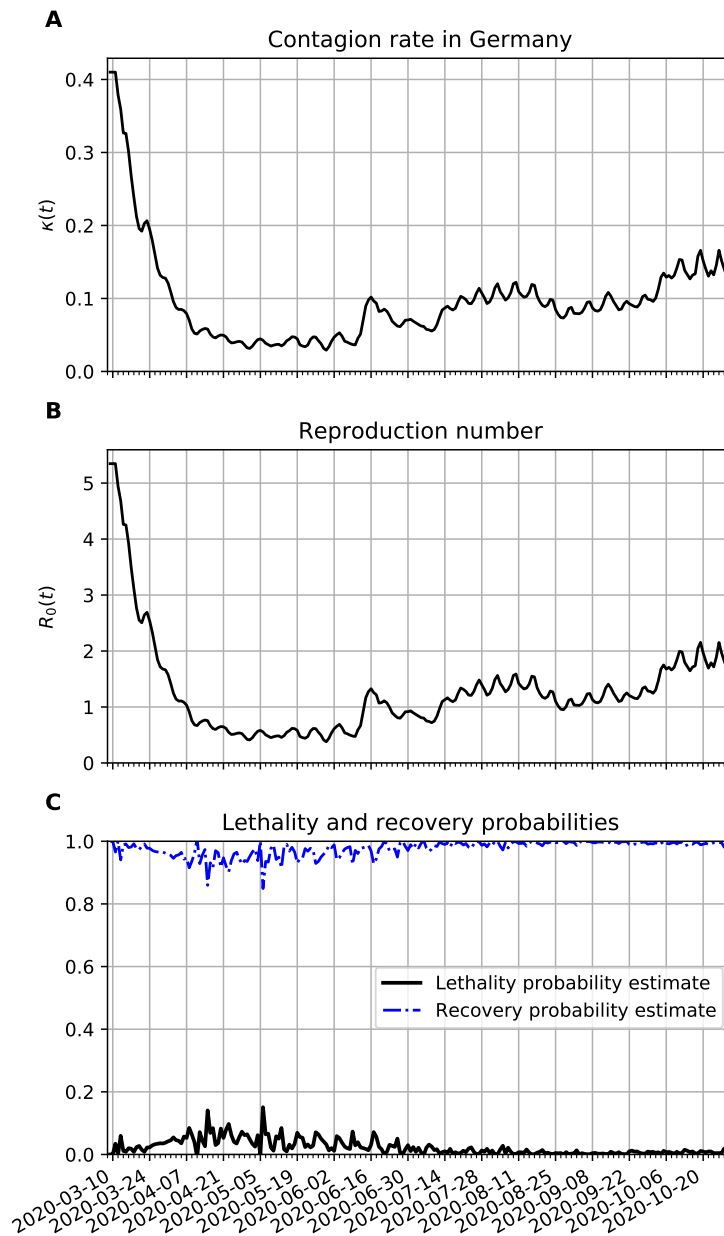


FIG. 4. Estimation of parameters of the epidemiological model. The initial date of the time series is the date in which the first death due to COVID-19 occurred in Germany. **A** the time variation of the contagion rate. The initial rate was very high, possibly due to exogenous cases in the early stages of the pandemic. To better fit the data with the predictions of our model we had to truncate $\kappa(t)$ with values above 0.41 at the beginning of the series. **B** the reproduction number. **C** the lethality and recovery rates.

B. Evolution of COVID-19 in Brazil

We consider the initial time the day of the first death case in Brazil. We take Brazil's population to be approximately $P_0 = 211.050 \times 10^6$. The initial date of the time series of the data

sets used is 03/20, one day after the first official death due to COVID-19 was recorded. We used the pre-pandemic birth and death rates shown in Table II. The estimates of contagion, lethality and recovery rates are obtained according to the methods described in Secs. III D 2 and III D 3, respectively. The time variation of the contagion rate reflects the fact that the population slowly took heed of the gravity of the pandemic and started adopting social distancing measures and using PPE.

In Fig. 5A, we compare the official data (blue dots) of confirmed cases with the corresponding time series obtained from our proposed model. In frame B, we show a comparison between the number of recovered cases (blue line) and the predicted number of recovered cases predicted by the theoretical model. The discrepancies in the fitting may have to do with delays in the confirmation of the recovered cases, as we can see in the jumps that occurred from 06/07 to 06/08 and from 07/01 to 07/02. One possible source of systematic error, towards sub-notification of recovered cases, could occur in milder cases. Also, recovered outpatients may fail to take another test to confirm their recoveries. In frame C, we show a comparison between the number of death cases due to COVID-19 (in blue) and the number of deaths predicted by the theoretical model. In frame D, we plot the active cases data along with the theoretical predictions based on our model. The theoretical fit is not as good as in the previous figures, but it is still quite reasonable. We again validate our forecasting model with a 95% confidence interval based on the Markov chain. In all cases the epidemiological data fell within the prediction range, but we had to backtrack 4 weeks in relation to the forecasting in Germany. The problem seems to be the artificial lack of report of new recoveries that can be seen in frame B.

In Fig. 6A, we show the time evolution of the contagion rate $\kappa(t)$. The sharp drop of this rate is likely due to the increase of isolation and social distancing that grew at the second half of March in Brazil. Since about 03/27 it has been decreasing slowly on average, despite the weekly modulations. This is certainly due to better precautions by the population (isolation, social distancing, hand washing, and the increased use of PPEs). In frame B, we plot the reproduction number as a function of time. It is basically a scaled version of $\kappa(t)$. Since about the beginning of July, $R_0(t)$ has been modulating around 1. Although, this is not enough since the number of active cases is still very high. In frame C, we show the time evolution of the lethality and recovery rates, $\lambda(t)$ and $\rho(t) = 1/\tau - \lambda(t)$, respectively. One sees more fluctuations near the beginning of the time series likely because there were less active cases then. Also, one sees that the lethality rate is decreasing on average. This might be related with the increased amount of testing in Brazil, which is still far below the necessary though. It could also be related with increased sub-notification of death

cases. Another possibility is that the medical treatment and procedures for the more severe cases of COVID-19 are being better treated since May. Whatever the case, this behavior should be further investigated.

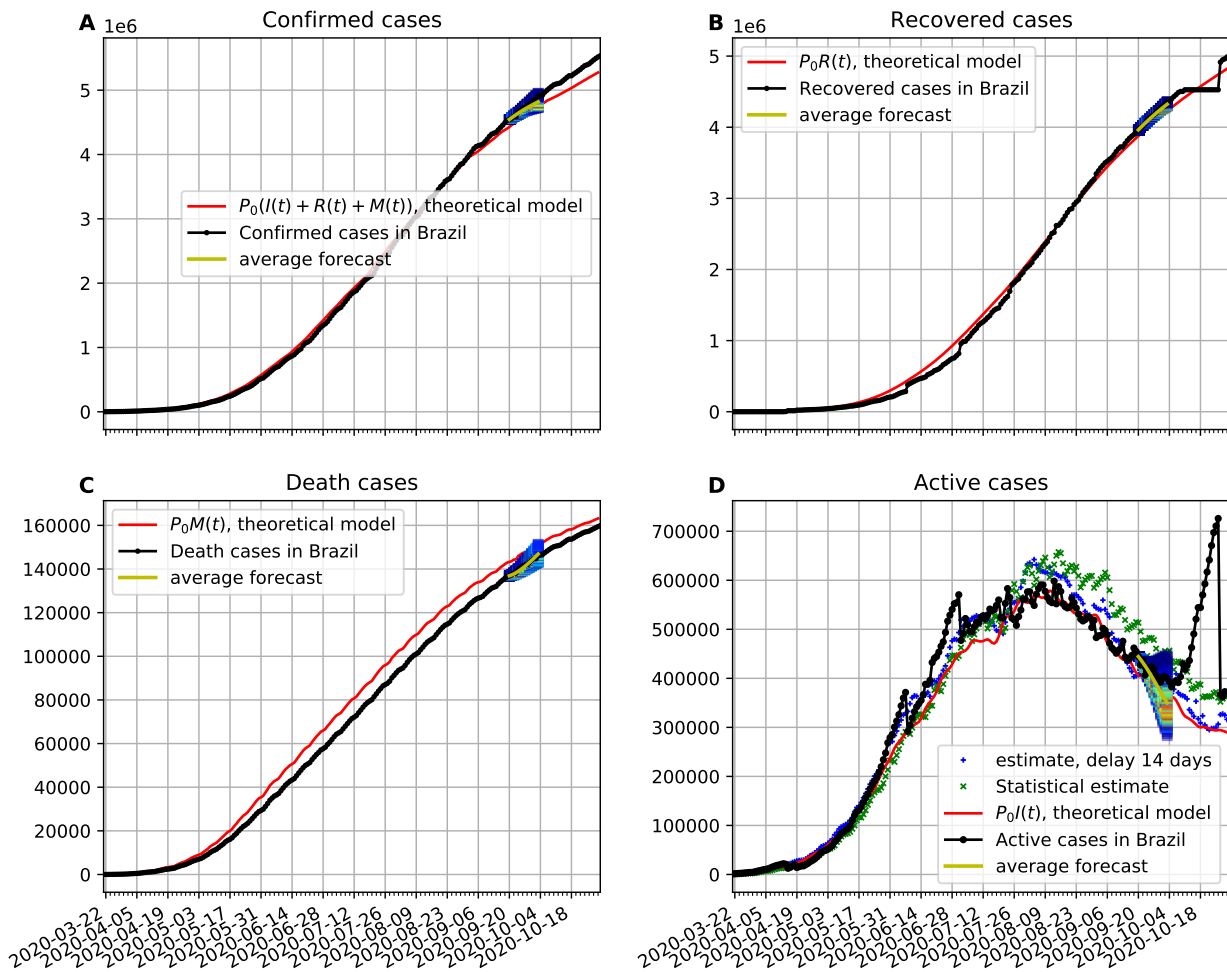


FIG. 5. **A** The number of official confirmed cases compared with the theoretical prediction. **B** Time evolution of the official number of recovered cases in comparison with the theoretical prediction. **C** The number of official deaths compared with the theoretical prediction. **D** The time evolution of the official number of active cases in Brazil compared with the theoretical prediction. In all cases the functions $\kappa(t)$, $\lambda(t)$, and $\rho(t)$ vary in time according to Fig. 6.

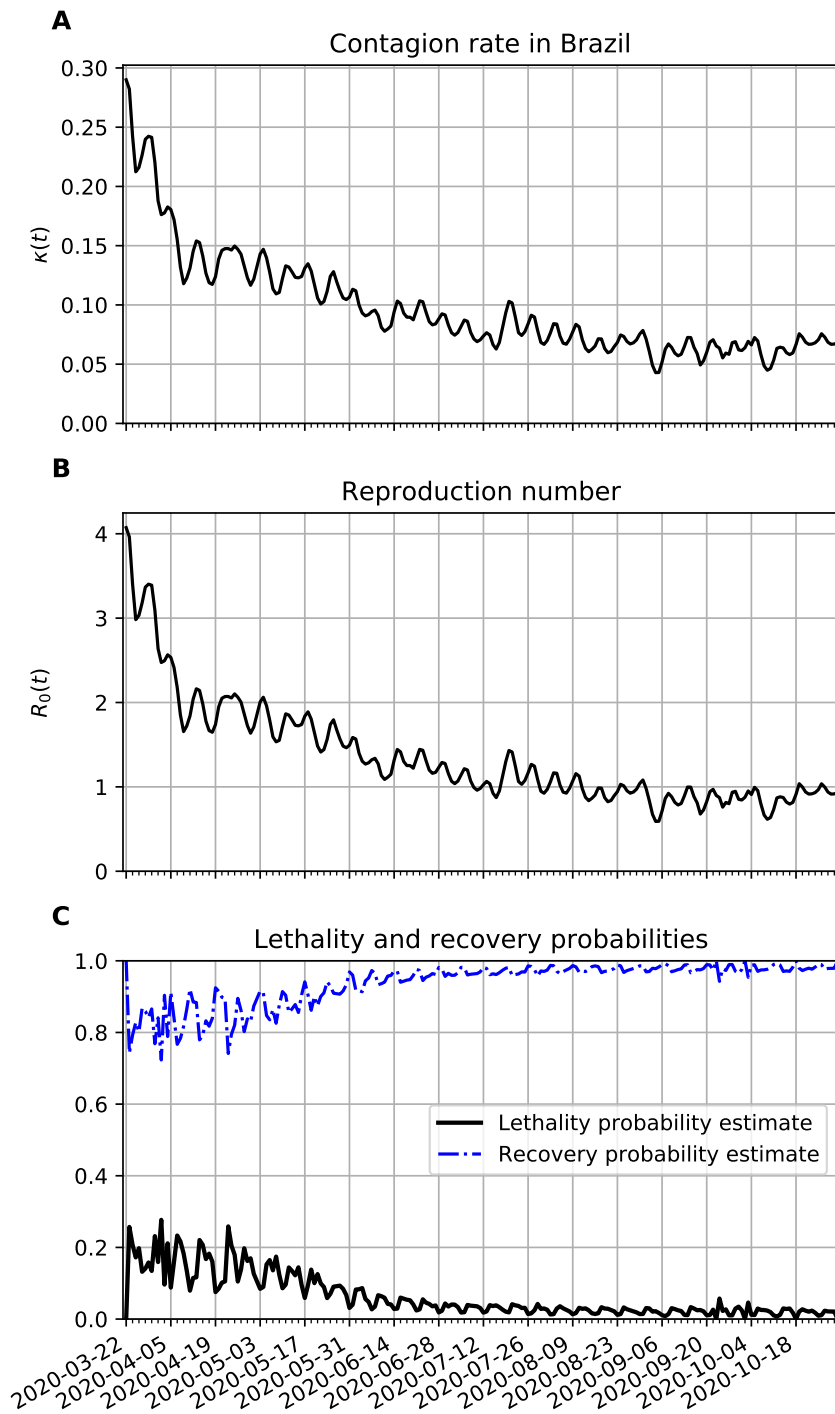


FIG. 6. **A** Time variation of the contagion rate in Brazil. This function was obtained from the statistically estimated active cases as described in Sec. III D 2. The oscillations reflect weekly variations that can be seen in the number of daily new cases. **B** Corresponding reproduction number evolution. **C** The lethality and recovery rates obtained with the method described in Sec. III D 3.

C. Evolution of COVID-19 in Paraíba

The initial population of Paraíba is $P_0 = 4,018,127$. The first case of COVID-19 contamination was registered on 03/18 and the first recorded death on 04/06. We did not plot the number of recovered cases because we have not been able, so far, to obtain this data for Paraíba.

In Fig. 7A, we compare the official data (blue dots) of confirmed cases with the corresponding time series obtained from our model. In frame B, we show a comparison between the number of death cases due to COVID-19 (blue line) and the number of deaths predicted by the theoretical model. In frame C, we show the estimated active cases. One result is based on delay and the other on the statistical method. Both methods are described in Sec. III C. We also show epidemiological model estimate (solid red line). Note also, that at the last two weeks of the time series we validate the forecasting model based on the Markov chain. Here, we show a 95% confidence band along two weeks. In this case the all epidemiological data fell well within the predictions.

In Fig. 8A, we show the time evolution of the contagion rate $\kappa(t)$. Initially, the contagion rate is not as high as in Brazil's case, but takes longer to drop. From about 04/06, the rate of contagion starts decreasing on average, although with a higher amplitude of modulation as in the case of Brazil. As time passes, one sees also a decrease in the amplitude of the modulations. This is certainly due to better precautions by the population (isolation, social distancing, hand washing, and the increased use of PPEs). In frame B, we plot the reproduction number as a function of time. It is basically a scaled version of $\kappa(t)$. Since about the beginning of July, $R_0(t)$ has been modulating around 1. Although, this is not enough to end the pandemic since the number of estimated active cases is still very high. In frame C, we show the time evolution of the lethality and recovery rates, $\lambda(t)$ and $\rho(t) = 1/\tau - \lambda(t)$, respectively. Again, one sees more fluctuations near the beginning of the time series likely because there were very few active cases then. Also, one sees that the lethality rate started decreasing on average after the first week of April. This might be related with the increased amount of testing in Paraíba, which is still far below the necessary though.

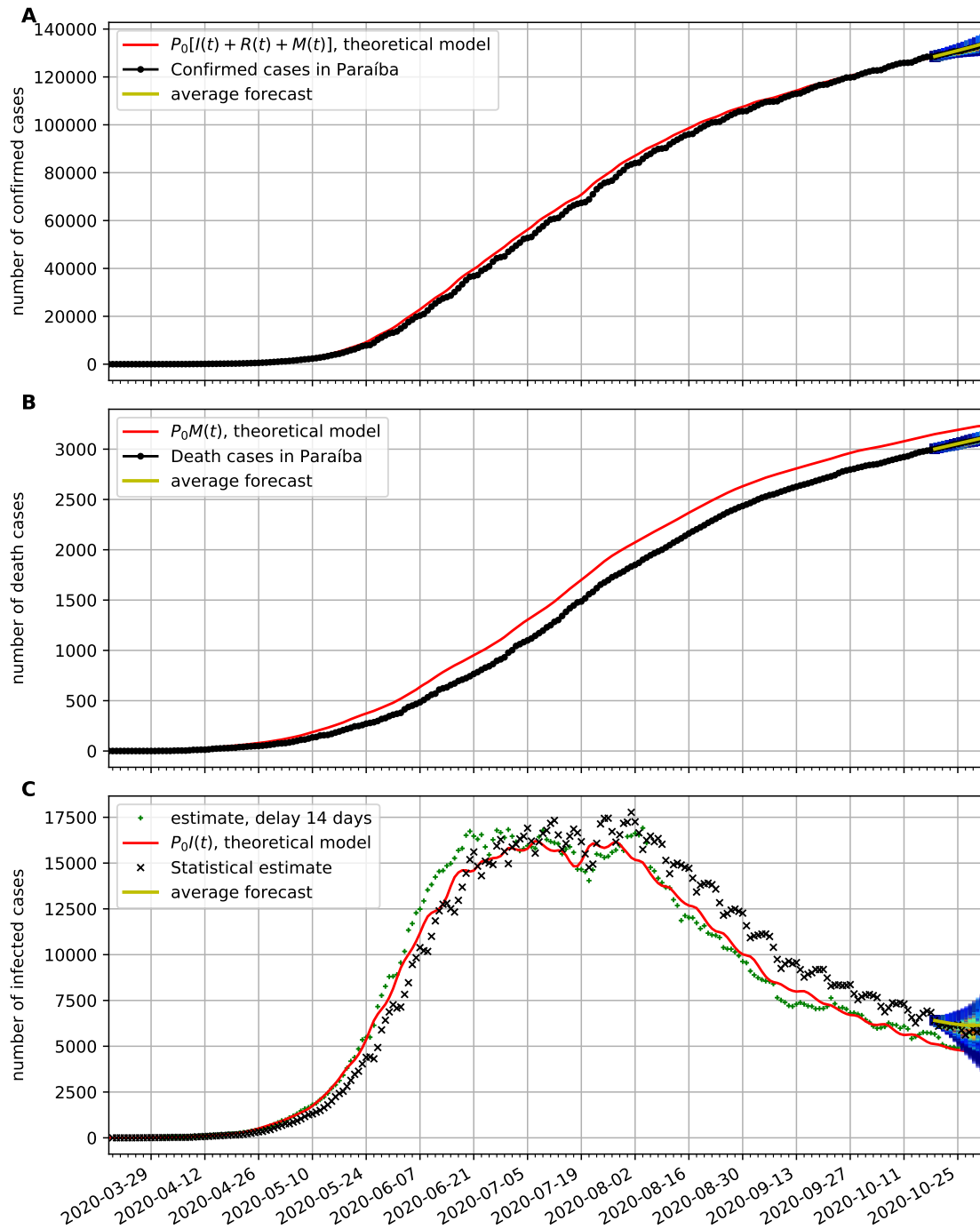


FIG. 7. The theoretical fit is obtained with $\tau = 13$ and the parameters estimated in Fig. 8. **A** Comparison of the number of official confirmed cases with the theoretical prediction. **B** Comparison of the number of official deaths due to COVID-19 infection with the theoretical prediction. **C** Comparison of the number of the estimated number of active cases with the theoretical prediction.

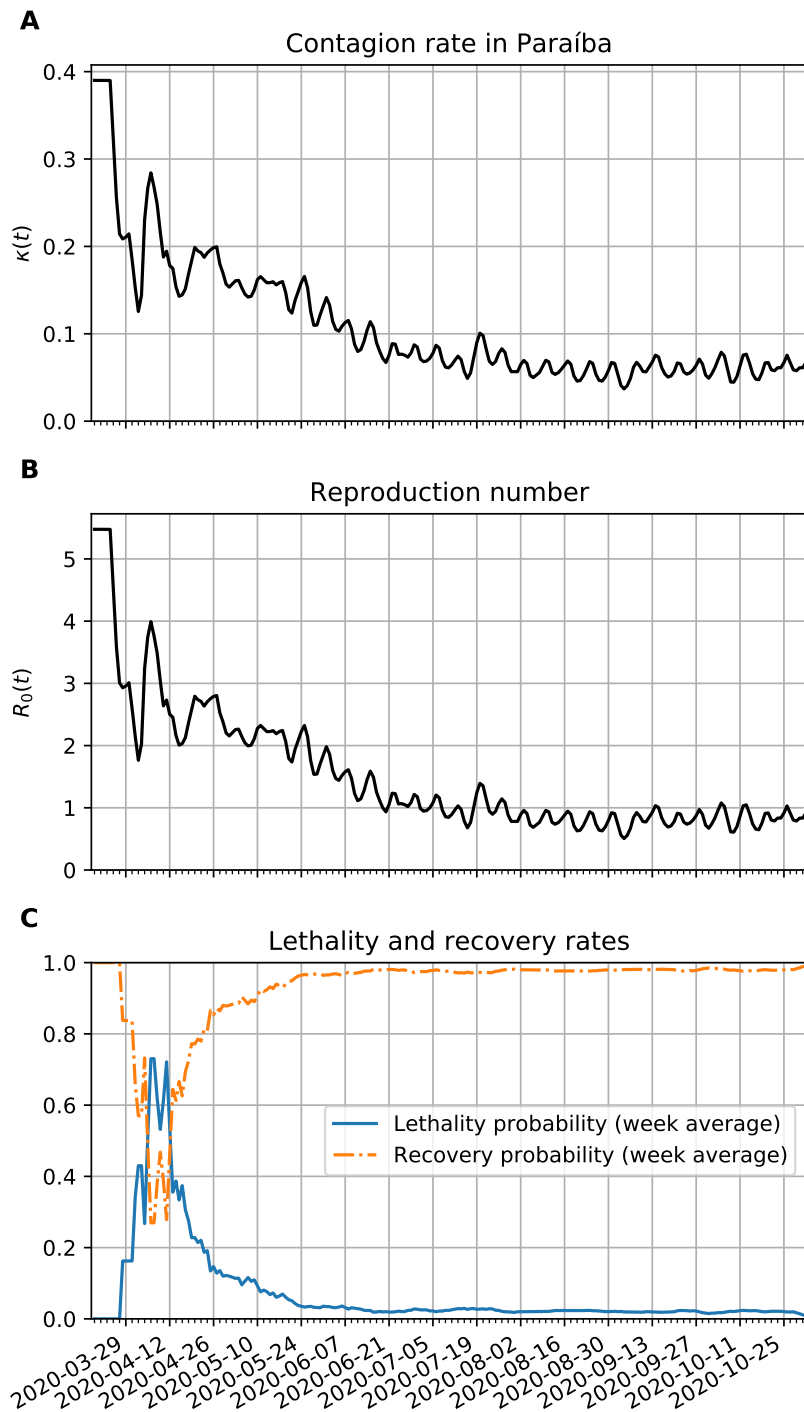


FIG. 8. **A** Time variation of the contagion rate in Paraíba. This function was obtained from the statistically estimated active cases described in Sec. III C and the method of Sec. III D 2. The initial cutoff value of $\kappa(t)$ is 0.38. **B** Corresponding reproduction number evolution. **C** Estimates for the lethality and recovery rates based on Sec. III D 3.

D. Evolution of COVID-19 in Campina Grande

The first case of COVID-19 contamination was registered on 03/27 and the first recorded death on 04/16. We did not plot the number of recovered cases because we have not been able, so far, to obtain this data for Campina Grande.

In Fig. 9A, we compare the official data (blue dots) of confirmed cases with the corresponding time series obtained from our model. In frame B, we show a comparison between the number of death cases due to COVID-19 (blue line) and the number of deaths predicted by the theoretical model. In frame C, we show the estimated active cases. One result is based on delay and the other on the statistical method. Both methods are described in Sec. III C. We also show the epidemiological model estimate (solid red line). Note also, that at the last two weeks of the time series we again validate the forecasting model based on the Markov chain. Here, we show a 95% confidence band along two weeks. In this case the all epidemiological data fell well within the predictions.

In Fig. 8A, we show the time evolution of the contagion rate $\kappa(t)$. Initially, the contagion rate is not as high as in Brazil's case, but takes longer to drop. Only from about 06/07, the rate of contagion starts decreasing on average, although with a higher amplitude of modulation as in the case of Brazil or Paraíba. As time passes, one sees also a decrease in the amplitude of the modulations. This is certainly due to better precautions by the population (isolation, social distancing, hand washing, and the increased use of PPEs). In frame B, we plot the reproduction number as a function of time. It is basically a scaled version of $\kappa(t)$. Since about the beginning of July, $R_0(t)$ has been modulating around 1. Although, this is not enough to end the pandemic since the number of estimated active cases is still very high. In frame C, we show the time evolution of the lethality and recovery rates, $\lambda(t)$ and $\rho(t) = 1/\tau - \lambda(t)$, respectively. Again, one sees more fluctuations near the beginning of the time series likely because there were very few active cases then. Also, one sees that the lethality rate started decreasing on average after the first week of April. This might be related with the increased amount of testing in Campina Grande, which is still far below the necessary though.

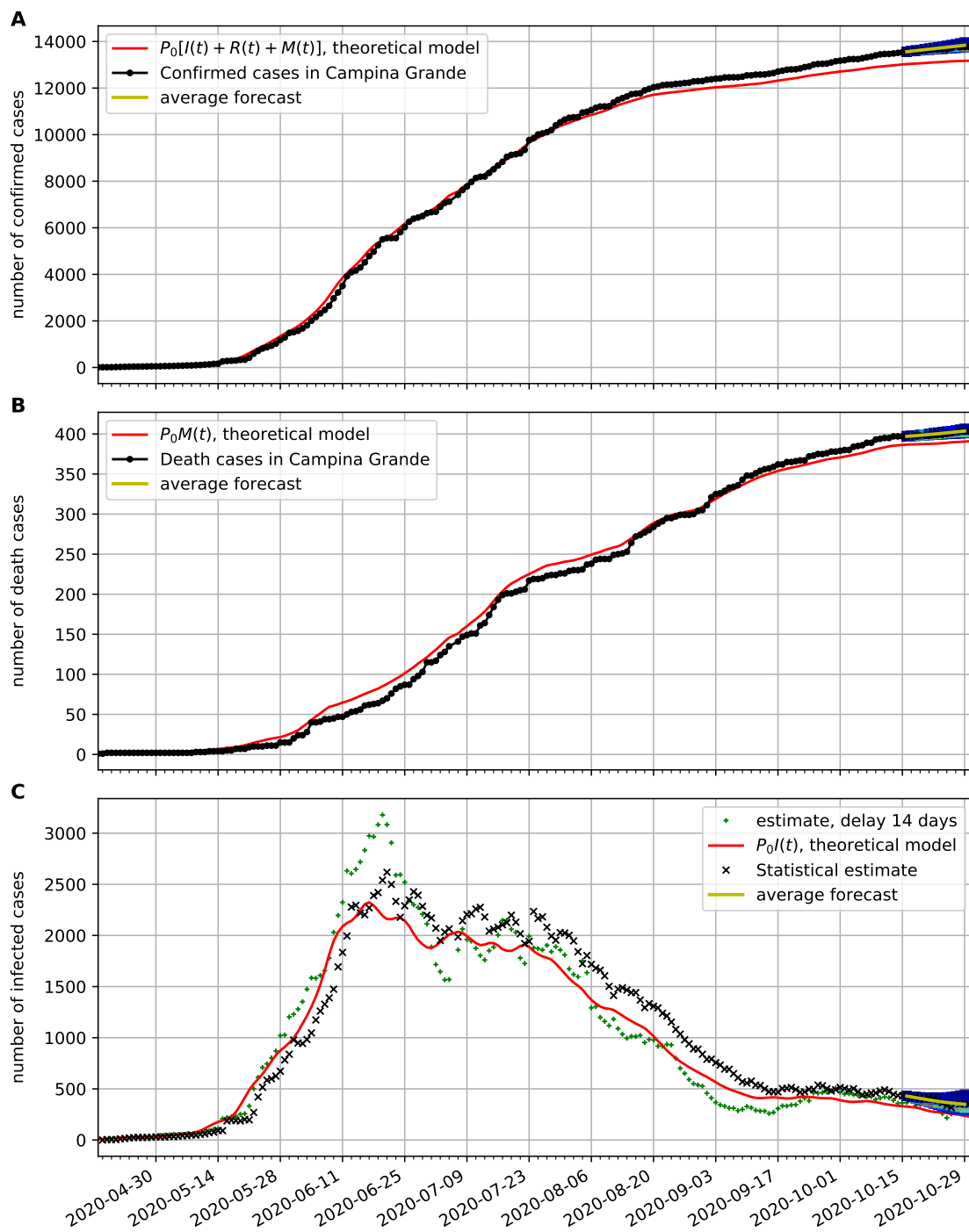


FIG. 9. The theoretical fit is obtained with $\tau = 14$ day and the parameters estimated in Fig. 10. **A** Comparison of the number of official confirmed cases with the theoretical prediction. **B** Comparison of the number of official deaths due to COVID-19 infection with the theoretical prediction. **C** Comparison of the number of the estimated number of active cases with the theoretical prediction.

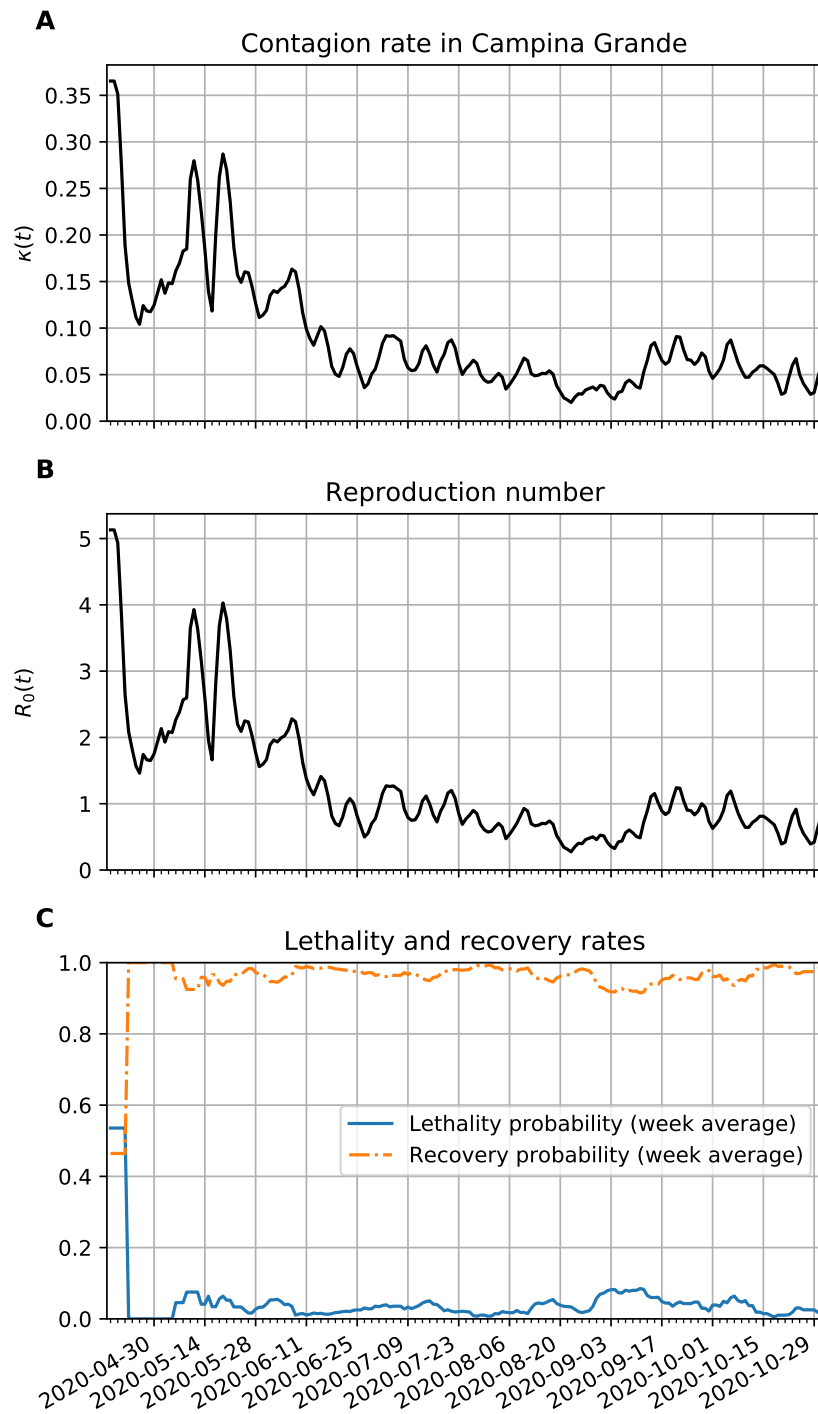


FIG. 10. **A** Time variation of the contagion rate in Paraíba. This function was obtained from the statistically estimated active cases described in Sec. III C and the method of Sec. III D 2. The initial cutoff value of $\kappa(t)$ is 0.3. **B** Corresponding reproduction number evolution. **C** Estimates for the lethality and recovery rates based on Sec. III D 3.

V. CONCLUSION

Here we summarize the main contributions of our epidemiological study of the evolution of the COVID-19 pandemic in four populations. The proposed model is an adaptation of the SIR model [4], a SIRD model [26], with some notable differences. In the SIRD model we replace the removed population by the recovered and the deceased. We allow that the contagion rate varies in time so that it reflects the fact that social distancing and isolation changes over time. We developed two ways to obtain the active population from the data on confirmed cases only. In the first approach, the number of active cases at time t is estimated simply by difference between the confirmed population at time t minus the confirmed population at time $t - \tau$, where τ denotes the average time span of infection. In the second approach, the number of active cases is estimated by the probabilistic model proposed here. Both approaches result in fairly accurate predictions of the active cases when the official data is available. In cases in which the data on recovered cases is not available, this approach could be the only way to estimate the number of active cases. We propose a new method to track automatically the contagion rate based on the statistical estimate of active cases. We divided the data in weekly intervals and for each interval we made a linear regression to obtain the slope, and based on the equation in our model for the infected, we could obtain a daily contagion rate. This contagion rate was fed back into the equations of motion and we were able to fit the data with a minimum of or no ad hoc interventions. We noticed that the contagion rate could reach very high values at the initial stages of the spread of the epidemic in all populations investigated. This likely happens because of inherent numerical errors, as described in Sec. III D 2, and multiple infections that are imported from contaminated visitors or people returning from trips abroad. This type of dynamics is more relevant at the beginning, when the local contaminated population is small and before barriers on travelling are imposed by the governments. Here, we also take into account the contribution from the pre-pandemic birth and death rates to the evolution of the populations investigated. This could become relevant if the pandemic lasts for over a year and also it is important as a comparison for the lethality of the pandemic. According to the results exposed in the previous section, with our model we could fit the official case data from Germany, Brazil, the State of Paraíba, and city of Campina Grande quite well.

The modeling of the spread of the pandemic in Germany is very emblematic, since it clearly shows that the strict social distancing measures imposed by the government on 03/22/2020 were very effective in containing the disease, reducing the R_0 from 2.8 down to roughly 1 about two weeks later, and further down to approximately 0.5 in more two weeks, according to our model.

In the case of Brazil, we conclude that, based on the fit of the proposed model, the decrease of the reproduction number has been far more difficult and bumpier. This means the implanted social distancing measures are having an effect in thwarting the spread of the disease, but it has not enough, since to control the pandemic since $R_0(t)$ has been oscillating around 1 and the number of active cases is still very high.

The evolution of COVID-19 in the State of Paraíba has been similar to the national case. The contagion rate has been decreasing on average, but the modulations are even bumpier than in the national case. The amplitude of the modulations is considerably higher than in Brazil. This may be due to the smaller population involved. The effective reproduction number has been decreasing on average but it is still hovering around 1, with an estimated large number of active cases.

As was commented in the Introduction, Campina Grande adopted a social distancing policy one week earlier than the report of the first confirmed case. Perhaps, due to this, the initial contagion rate was lower than the corresponding ones in Brazil and Paraíba. Despite of this, the rate of contagion did not decrease as fast as it did in Germany, Brazil or even in Paraíba. It presents two major peaks in $\kappa(t)$ spaced apart by a week since the outbreak of the disease here. Probably these could be linked to agglomeration events such as in-branch governmental relief payments to unemployed people. Also, one sees higher amplitude of the modulation of the contagion rate than in the other populations studied, this might be linked to the smaller size of the population involved.

We also proposed and validated a simple forecasting method based on Markov chains and on our parameter estimation method for the evolution of the epidemiological data for up to two weeks. For the populations we investigated, the epidemiological data fell well within the 95% confidence interval of our predictions.

Based on the results shown here, we conclude that the public health officials should look into the local dynamics of the spread of the disease as they compare with the theoretical predictions of models such as the one developed here. In this way, they will know where the social distancing and isolation is being more efficiently implemented. The models will be more relevant and accurate if there is more testing of the population. Even random testing should be considered, as one gains statistical information on the spread of the disease and discovers where there is more under-notification. Also, cellphone data of the motion of the population, as used by Peixoto *et al.* [27] and Linka *et al.* [15], should be considered as a means of predicting the contagion and of identifying hot spots of COVID-19. This could help identify where there are more contagions: bars, churches, supermarkets, offices, pharmacies, hospitals, bakeries, restaurants, by delivery services, or family visits, etc. Furthermore, by comparing different local strategies one could gain insight on what

works better for slowing the spread of the disease. It would be interesting to see the amount of correlation in population mobility and contagion rate, this could be specially relevant at the city level. In a more refined work, one could couple several nearby cities into a network of populations.

-
- [1] “Coronavirus disease 2019 (COVID-19) situation report –41,” https://www.who.int/docs/default-source/coronaviruse/situation-reports/20200301-sitrep-41-covid-19.pdf?sfvrsn=6768306d_2 (2020), accessed on 06/15/2020.
- [2] David S Hui, Esam I Azhar, Tariq A Madani, Francine Ntoumi, Richard Kock, Osman Dar, Giuseppe Ippolito, Timothy D Mchugh, Ziad A Memish, Christian Drosten, Alimuddin Zumla, and Eskild Petersen, “The continuing 2019-nCoV epidemic threat of novel coronaviruses to global health: The latest 2019 novel coronavirus outbreak in Wuhan, China,” *International Journal of Infectious Diseases* **91**, 264–266 (2020).
- [3] “Who director-general’s opening remarks at the media briefing on COVID-19 - 11 march 2020,” <https://www.who.int/dg/speeches/detail/who-director-general-s-opening-remarks-at-the-media-briefing-on-covid-19---11-march-2020> (2020), accessed on 05/27/2020.
- [4] William O Kermack and Anderson G McKendrick, “A contribution to the mathematical theory of epidemics,” *Proceedings of the Royal Society of London. Series A* **115**, 700–721 (1927).
- [5] G Gómez Alcaraz and C Vargas-De-León, “Modeling control strategies for influenza A H1N1 epidemics: SIR models,” *Revista Mexicana de Física* **58**, 37–43 (2012).
- [6] Saulo B Bastos and Daniel O Cajueiro, “Modeling and forecasting the COVID-19 pandemic in Brazil,” arXiv preprint [arXiv:2003.14288](https://arxiv.org/abs/2003.14288) (2020).
- [7] Raúl Isea and Karl E Lonngren, “On the mathematical interpretation of epidemics by Kermack and McKendrick,” *Gen. Math. Notes.* **19**, 83–87 (2013).
- [8] Nuno Crokidakis, “Data analysis and modeling of the evolution of COVID-19 in Brazil,” arXiv preprint [arXiv:2003.12150](https://arxiv.org/abs/2003.12150) (2020).
- [9] F Ndairou, I Area, J Nieto, and D F M Torres, “Mathematical modeling of COVID-19 transmission dynamics with a case study of Wuhan,” *Chaos, Solitons and Fractals* **135**, 1–6 (2020).
- [10] Alexandra Smirnova, Linda deCamp, and Gerardo Chowell, “Forecasting epidemics through nonparametric estimation of time-dependent transmission rates using the SEIR model,” *Bulletin of Mathematical Biology* **81**, 4343–4365 (2019).

- [11] Y Fang, Y Nie, and M Penny, “Transmission dynamics of the COVID-19 outbreak and effectiveness of government interventions: A data-driven analysis,” *Journal of Medical Virology* **92**, 645–659 (2020).
- [12] Linhao Zhong, Lin Mu, Jing Li, Jiaying Wang, Zhe Yin, and Darong Liu, “Early prediction of the 2019 novel coronavirus outbreak in the mainland China based on simple mathematical model,” *IEEE Access* **8**, 51761–51769 (2020).
- [13] Yi-Cheng Chen, Ping-En Lu, and Cheng-Shang Chang, “A time-dependent SIR model for COVID-19,” arXiv preprint [arXiv:2003.00122](https://arxiv.org/abs/2003.00122) (2020).
- [14] Jonas Dehning, Johannes Zierenberg, F Paul Spitzner, Michael Wibral, Joao Pinheiro Neto, Michael Wilczek, and Viola Priesemann, “Inferring change points in the spread of COVID-19 reveals the effectiveness of interventions,” *Science* **369** (2020), [10.1126/science.abb9789](https://doi.org/10.1126/science.abb9789).
- [15] K Linka, A Goriely, and E Kuhl, “Global and local mobility as a barometer for COVID-19 dynamics,” *medRxiv*, 1–26 (2020).
- [16] Andrea L. Bertozzi, Elisa Franco, George Mohler, Martin B. Short, and Daniel Sledge, “The challenges of modeling and forecasting the spread of covid-19,” *Proceedings of the National Academy of Sciences* **117**, 16732–16738 (2020).
- [17] Severino H da Silva, “Asymptotic behavior for a non-autonomous model of neural fields with variable external stimuli,” .
- [18] O Diekmann and Ph Getto, “Boundedness, global existence and continuous dependence for nonlinear dynamical systems describing physiologically structured populations,” *Journal of Differential Equations* **215** (2005), DOI: [10.1016/j.jde.2004.10.025](https://doi.org/10.1016/j.jde.2004.10.025).
- [19] Adriano A Batista and Severino H Da Silva, “an epidemiological compartmental model with automated parameter estimation of the spread of covid-19 with analysis of data from germany and brazil,” .
- [20] J K Hale, *Ordinary Differential Equations* (Dover, 2009).
- [21] James D Murray, *Mathematical Biology: I. An Introduction*, Vol. 17 (Springer Science & Business Media, 2007).
- [22] Statistisches Bundesamt, “[Daten der lebendgeborenen, totgeborenen, gestorbenen und der gestorbenen im 1. lebensjahr,](#)” (), accessed on 06/15/2020.
- [23] Statistisches Bundesamt, “[Sterbefälle und lebenserwartung,](#)” (), accessed on 06/15/2020.
- [24] Pauli Virtanen *et al.*, “SciPy 1.0: Fundamental Algorithms for Scientific Computing in Python,” *Nature Methods* **17**, 261–272 (2020).
- [25] Deutsche Welle, “[What are Germany’s new coronavirus social distancing rules?](#)” Accessed on 07/23/2020.

- [26] Herbert W Hethcote, “The mathematics of infectious diseases,” *SIAM review* **42**, 599–653 (2000).
- [27] PS Peixoto et al., “Potential dissemination of epidemics based on Brazilian mobile geolocation data. Part I: Population dynamics and future spreading of infection in the states of São Paulo and Rio de Janeiro during the pandemic of COVID-19,” [medRxiv](#), 1–18 (2020).